Fermi National Accelerator Laboratory

FERMILAB-Conf-96/248-E
D0

The $b\bar{b}$ Production Cross Section and Correlations in $p\bar{p}$ Collisions at $\sqrt{s}$ = 1.8 TeV

S. Abachi et al.
The D0 Collaboration

Fermi National Accelerator Laboratory
P.O. Box 500, Batavia, Illinois 60510

August 1996

Submitted to the *28th International Conference on High Energy Physics (ICHEP96)*,
Warsaw, Poland, July 25-31, 1996

Operated by Universities Research Association Inc. under Contract No. DE-AC02-76CHO3000 with the United States Department of Energy

Disclaimer

This report was prepared as an account of work sponsored by an agency of the United States Government. Neither the United States Government nor any agency thereof, nor any of their employees, makes any warranty, expressed or implied, or assumes any legal liability or responsibility for the accuracy, completeness, or usefulness of any information, apparatus, product, or process disclosed, or represents that its use would not infringe privately owned rights. Reference herein to any specific commercial product, process, or service by trade name, trademark, manufacturer, or otherwise, does not necessarily constitute or imply its endorsement, recommendation, or favoring by the United States Government or any agency thereof. The views and opinions of authors expressed herein do not necessarily state or reflect those of the United States Government or any agency thereof.

Distribution

Approved for public release; further dissemination unlimited.

FERMILAB Conf-96/248-E

The $b\overline{b}$ Production Cross Section and Correlations in $p\overline{p}$ Collisions at $\sqrt{s} = 1.8$ TeV

The DØ Collaboration[1]

(July 1996)

We present measurements of the $b\overline{b}$ production cross section and angular correlations between the b and $\overline{b}$-quarks in $p\overline{p}$ collisions using the DØ detector at the Fermilab Tevatron operating at $\sqrt{s} = 1.8$ TeV. The b-quark production cross section for $|y^b| < 1.0$ and $p_T^b > 8$ GeV/c is extracted and found to be consistent with next-to-leading order QCD predictions. In addition, the angular correlations between the b and $\overline{b}$-quarks are found to agree in shape with next-to-leading order QCD predictions.

S. Abachi,[14] B. Abbott,[28] M. Abolins,[25] B.S. Acharya,[43] I. Adam,[12] D.L. Adams,[37] M. Adams,[17] S. Ahn,[14] H. Aihara,[22] J. Alitti,[40] G. Álvarez,[18] G.A. Alves,[10] E. Amidi,[29] N. Amos,[24] E.W. Anderson,[19] S.H. Aronson,[4] R. Astur,[42] R.E. Avery,[31] M.M. Baarmand,[42] A. Baden,[23] V. Balamurali,[32] J. Balderston,[16] B. Baldin,[14] S. Banerjee,[43] J. Bantly,[5] J.F. Bartlett,[14] K. Bazizi,[39] J. Bendich,[22] S.B. Beri,[34] I. Bertram,[37] V.A. Bezzubov,[35] P.C. Bhat,[14] V. Bhatnagar,[34] M. Bhattacharjee,[13] A. Bischoff,[9] N. Biswas,[32] G. Blazey,[14] S. Blessing,[15] P. Bloom,[7] A. Boehnlein,[14] N.I. Bojko,[35] F. Borcherding,[14] J. Borders,[39] C. Boswell,[9] A. Brandt,[14] R. Brock,[25] A. Bross,[14] D. Buchholz,[31] V.S. Burtovoi,[35] J.M. Butler,[3] W. Carvalho,[10] D. Casey,[39] H. Castilla-Valdez,[11] D. Chakraborty,[42] S.-M. Chang,[29] S.V. Chekulaev,[35] L.-P. Chen,[22] W. Chen,[42] S. Choi,[41] S. Chopra,[24] B.C. Choudhary,[9] J.H. Christenson,[14] M. Chung,[17] D. Claes,[42] A.R. Clark,[22] W.G. Cobau,[23] J. Cochran,[9] W.E. Cooper,[14] C. Cretsinger,[39] D. Cullen-Vidal,[5] M.A.C. Cummings,[16] D. Cutts,[5] O.I. Dahl,[22] K. De,[44] M. Demarteau,[14] N. Denisenko,[14] D. Denisov,[14] S.P. Denisov,[35] H.T. Diehl,[14] M. Diesburg,[14] G. Di Loreto,[25] R. Dixon,[14] P. Draper,[44] J. Drinkard,[8] Y. Ducros,[40] S.R. Dugad,[43] D. Edmunds,[25] J. Ellison,[9] V.D. Elvira,[42] R. Engelmann,[42] S. Eno,[23] G. Eppley,[37] P. Ermolov,[26] O.V. Eroshin,[35] V.N. Evdokimov,[35] S. Fahey,[25] T. Fahland,[5] M. Fatyga,[4] M.K. Fatyga,[39] J. Featherly,[4] S. Feher,[14] D. Fein,[2] T. Ferbel,[39] G. Finocchiaro,[42] H.E. Fisk,[14] Y. Fisyak,[7] E. Flattum,[25] G.E. Forden,[2] M. Fortner,[30] K.C. Frame,[25] P. Franzini,[12] S. Fuess,[14] E. Gallas,[44] A.N. Galyaev,[35] T.L. Geld,[25] R.J. Genik II,[25] K. Genser,[14] C.E. Gerber,[14] B. Gibbard,[4] V. Glebov,[39] S. Glenn,[7] J.F. Glicenstein,[40] B. Gobbi,[31] M. Goforth,[15] A. Goldschmidt,[22] B. Gómez,[1] G. Gomez,[23] P.I. Goncharov,[35] J.L. González Solís,[11] H. Gordon,[4] L.T. Goss,[45] N. Graf,[4] P.D. Grannis,[42] D.R. Green,[14] J. Green,[30] H. Greenlee,[14] G. Griffin,[8] N. Grossman,[14] P. Grudberg,[22] S. Grünendahl,[39] W.X. Gu,[14,*] G. Guglielmo,[33] J.A. Guida,[2] J.M. Guida,[5] W. Guryn,[4] S.N. Gurzhiev,[35] P. Gutierrez,[33] Y.E. Gutnikov,[35] N.J. Hadley,[23] H. Haggerty,[14] S. Hagopian,[15] V. Hagopian,[15] K.S. Hahn,[39] R.E. Hall,[8] S. Hansen,[14] R. Hatcher,[25] J.M. Hauptman,[19] D. Hedin,[30] A.P. Heinson,[9] U. Heintz,[14] R. Hernández-Montoya,[11] T. Heuring,[15] R. Hirosky,[15] J.D. Hobbs,[14] B. Hoeneisen,[1,†]

[1]Submitted to the 28th International Conference on High Energy Physics, Warsaw, Poland, 25-31 July 1996.

J.S. Hoftun,[5] F. Hsieh,[24] Tao Hu,[14,*] Ting Hu,[42] Tong Hu,[18] T. Huehn,[9] S. Igarashi,[14] A.S. Ito,[14] E. James,[2] J. Jaques,[32] S.A. Jerger,[25] J.Z.-Y. Jiang,[42] T. Joffe-Minor,[31] H. Johari,[29] K. Johns,[2] M. Johnson,[14] H. Johnstad,[29] A. Jonckheere,[14] M. Jones,[16] H. Jöstlein,[14] S.Y. Jun,[31] C.K. Jung,[42] S. Kahn,[4] G. Kalbfleisch,[33] J.S. Kang,[20] R. Kehoe,[32] M.L. Kelly,[32] L. Kerth,[22] C.L. Kim,[20] S.K. Kim,[41] A. Klatchko,[15] B. Klima,[14] B.I. Klochkov,[35] C. Klopfenstein,[7] V.I. Klyukhin,[35] V.I. Kochetkov,[35] J.M. Kohli,[34] D. Koltick,[36] A.V. Kostritskiy,[35] J. Kotcher,[4] J. Kourlas,[28] A.V. Kozelov,[35] E.A. Kozlovski,[35] M.R. Krishnaswamy,[43] S. Krzywdzinski,[14] S. Kunori,[23] S. Lami,[42] G. Landsberg,[14] J-F. Lebrat,[40] A. Leflat,[26] H. Li,[42] J. Li,[44] Y.K. Li,[31] Q.Z. Li-Demarteau,[14] J.G.R. Lima,[38] D. Lincoln,[24] S.L. Linn,[15] J. Linnemann,[25] R. Lipton,[14] Y.C. Liu,[31] F. Lobkowicz,[39] S.C. Loken,[22] S. Lökös,[42] L. Lueking,[14] A.L. Lyon,[23] A.K.A. Maciel,[10] R.J. Madaras,[22] R. Madden,[15] L. Magaña-Mendoza,[11] S. Mani,[7] H.S. Mao,[14,*] R. Markeloff,[30] L. Markosky,[2] T. Marshall,[18] M.I. Martin,[14] B. May,[31] A.A. Mayorov,[35] R. McCarthy,[42] T. McKibben,[17] J. McKinley,[25] T. McMahon,[33] H.L. Melanson,[14] J.R.T. de Mello Neto,[38] K.W. Merritt,[14] H. Miettinen,[37] A. Mincer,[28] J.M. de Miranda,[10] C.S. Mishra,[14] N. Mokhov,[14] N.K. Mondal,[43] H.E. Montgomery,[14] P. Mooney,[1] H. da Motta,[10] M. Mudan,[28] C. Murphy,[17] F. Nang,[5] M. Narain,[14] V.S. Narasimham,[43] A. Narayanan,[2] H.A. Neal,[24] J.P. Negret,[1] E. Neis,[24] P. Nemethy,[28] D. Nešić,[5] M. Nicola,[10] D. Norman,[45] L. Oesch,[24] V. Oguri,[38] E. Oltman,[22] N. Oshima,[14] D. Owen,[25] P. Padley,[37] M. Pang,[19] A. Para,[14] C.H. Park,[14] Y.M. Park,[21] R. Partridge,[5] N. Parua,[43] M. Paterno,[39] J. Perkins,[44] A. Peryshkin,[14] M. Peters,[16] H. Piekarz,[15] Y. Pischalnikov,[36] V.M. Podstavkov,[35] B.G. Pope,[25] H.B. Prosper,[15] S. Protopopescu,[4] D. Pušeljić,[22] J. Qian,[24] P.Z. Quintas,[14] R. Raja,[14] S. Rajagopalan,[42] O. Ramirez,[17] M.V.S. Rao,[43] P.A. Rapidis,[14] L. Rasmussen,[42] S. Reucroft,[29] M. Rijssenbeek,[42] T. Rockwell,[25] N.A. Roe,[22] P. Rubinov,[31] R. Ruchti,[32] J. Rutherfoord,[2] A. Sánchez-Hernández,[11] A. Santoro,[10] L. Sawyer,[44] R.D. Schamberger,[42] H. Schellman,[31] J. Sculli,[28] E. Shabalina,[26] C. Shaffer,[15] H.C. Shankar,[43] R.K. Shivpuri,[13] M. Shupe,[2] J.B. Singh,[34] V. Sirotenko,[30] W. Smart,[14] A. Smith,[2] R.P. Smith,[14] R. Snihur,[31] G.R. Snow,[27] J. Snow,[33] S. Snyder,[4] J. Solomon,[17] P.M. Sood,[34] M. Sosebee,[44] M. Souza,[10] A.L. Spadafora,[22] R.W. Stephens,[44] M.L. Stevenson,[22] D. Stewart,[24] D.A. Stoianova,[35] D. Stoker,[8] K. Streets,[28] M. Strovink,[22] A. Sznajder,[10] P. Tamburello,[23] J. Tarazi,[8] M. Tartaglia,[14] T.L. Taylor,[31] J. Thompson,[23] T.G. Trippe,[22] P.M. Tuts,[12] N. Varelas,[25] E.W. Varnes,[22] P.R.G. Virador,[22] D. Vititoe,[2] A.A. Volkov,[35] A.P. Vorobiev,[35] H.D. Wahl,[15] G. Wang,[15] J. Warchol,[32] G. Watts,[5] M. Wayne,[32] H. Weerts,[25] A. White,[44] J.T. White,[45] J.A. Wightman,[19] J. Wilcox,[29] S. Willis,[30] S.J. Wimpenny,[9] J.V.D. Wirjawan,[45] J. Womersley,[14] E. Won,[39] D.R. Wood,[29] H. Xu,[5] R. Yamada,[14] P. Yamin,[4] C. Yanagisawa,[42] J. Yang,[28] T. Yasuda,[29] P. Yepes,[37] C. Yoshikawa,[16] S. Youssef,[15] J. Yu,[14] Y. Yu,[41] Q. Zhu,[28] Z.H. Zhu,[39] D. Zieminska,[18] A. Zieminski,[18] E.G. Zverev,[26] and A. Zylberstejn[40]

[1]Universidad de los Andes, Bogotá, Colombia
[2]University of Arizona, Tucson, Arizona 85721
[3]Boston University, Boston, Massachusetts 02215
[4]Brookhaven National Laboratory, Upton, New York 11973
[5]Brown University, Providence, Rhode Island 02912
[6]Universidad de Buenos Aires, Buenos Aires, Argentina
[7]University of California, Davis, California 95616
[8]University of California, Irvine, California 92717
[9]University of California, Riverside, California 92521
[10]LAFEX, Centro Brasileiro de Pesquisas Físicas, Rio de Janeiro, Brazil
[11]CINVESTAV, Mexico City, Mexico
[12]Columbia University, New York, New York 10027
[13]Delhi University, Delhi, India 110007
[14]Fermi National Accelerator Laboratory, Batavia, Illinois 60510

[15]Florida State University, Tallahassee, Florida 32306
[16]University of Hawaii, Honolulu, Hawaii 96822
[17]University of Illinois at Chicago, Chicago, Illinois 60607
[18]Indiana University, Bloomington, Indiana 47405
[19]Iowa State University, Ames, Iowa 50011
[20]Korea University, Seoul, Korea
[21]Kyungsung University, Pusan, Korea
[22]Lawrence Berkeley National Laboratory and University of California, Berkeley, California 94720
[23]University of Maryland, College Park, Maryland 20742
[24]University of Michigan, Ann Arbor, Michigan 48109
[25]Michigan State University, East Lansing, Michigan 48824
[26]Moscow State University, Moscow, Russia
[27]University of Nebraska, Lincoln, Nebraska 68588
[28]New York University, New York, New York 10003
[29]Northeastern University, Boston, Massachusetts 02115
[30]Northern Illinois University, DeKalb, Illinois 60115
[31]Northwestern University, Evanston, Illinois 60208
[32]University of Notre Dame, Notre Dame, Indiana 46556
[33]University of Oklahoma, Norman, Oklahoma 73019
[34]University of Panjab, Chandigarh 16-00-14, India
[35]Institute for High Energy Physics, 142-284 Protvino, Russia
[36]Purdue University, West Lafayette, Indiana 47907
[37]Rice University, Houston, Texas 77251
[38]Universidade Estadual do Rio de Janeiro, Brazil
[39]University of Rochester, Rochester, New York 14627
[40]CEA, DAPNIA/Service de Physique des Particules, CE-SACLAY, France
[41]Seoul National University, Seoul, Korea
[42]State University of New York, Stony Brook, New York 11794
[43]Tata Institute of Fundamental Research, Colaba, Bombay 400005, India
[44]University of Texas, Arlington, Texas 76019
[45]Texas A&M University, College Station, Texas 77843

INTRODUCTION

Measurements of the b-quark production cross section and $b\overline{b}$ correlations in $p\overline{p}$ collisions provide an important test of perturbative QCD at next-to-leading order (NLO). The measured b-quark production cross section (1) is in agreement with the NLO QCD predictions (2,3). The central values of the data lie a factor of approximately 2 above the central values of the theoretical predictions but the two are in agreement within experimental and theoretical uncertainties. Measurement of $b\overline{b}$ correlations such as the difference in azimuthal angle between the b and the $\overline{b}$-quarks allow additional details of b-quark production to be tested since these quantities are sensitive to the relative amounts of different production mechanisms.

This analysis makes use of the fact that the semi-leptonic decay of a b-quark results in a lepton(a muon in this analysis) plus an associated jet. We measure both the b-quark production cross section and the angular correlations between the $b\overline{b}$ pair starting with a sample of dimuons and their associated jets to tag both the b and $\overline{b}$-quarks.

DETECTOR AND EVENT SELECTION

The DØ detector and trigger system are described in detail elsewhere (4). The central muon system consists of 3 layers of proportional drift tubes and a magnetized iron toroid located between the first two layers. The muon detector provides a measurement of the muon momentum with a resolution parameterized by $\delta(1/p)/(1/p) = 0.18(p-2)/p \oplus 0.008p$, with p in GeV/c. The calorimeter is used to measure both the minimum ionizing energy associated with the muon track and the electromagnetic and hadronic activity associated with heavy quark decay. The total thickness of the calorimeter plus toroid in the central region varies from 13 to 15 interaction lengths which reduces the hadronic punchthrough in the muon system to less than 0.5% of all sources of low transverse momentum muons. The energy resolution for jets is $\approx 80\%/\sqrt{E(\mathrm{GeV})}$.

The data used in this analysis was taken during the 1992-1993 run of the Fermilab Tevatron collider and corresponds to a total integrated luminosity $\int \mathcal{L}dt = 6.5 \pm 0.4$ pb^{-1}. The dimuon data was collected using a multilevel trigger requiring at least one reconstructed muon with transverse momentum $p_T^\mu > 3$ GeV/c and at least one reconstructed jet with transverse energy $E_T > 10$ GeV. The events were then fully reconstructed offline and subjected to further cuts. The offline analysis required two muons with $p_T^\mu > 4$ GeV/c and pseudorapidity $|\eta^\mu| < 0.8$. Both muon tracks were required to be consistent with the reconstructed event vertex and to deposit > 1 GeV of energy in the calorimeter. Each muon was also required to have an associated jet with $E_T > 12$ GeV within a cone of $\Delta R = \sqrt{(\Delta\eta)^2 + (\Delta\phi)^2} < 0.8$. In addition, muon candidates in the region $80° < \varphi^\mu < 110°$ were excluded due to poorly measured chamber efficiencies around the Main Ring beam pipe.

Further cuts are also placed on the dimuon system to reduce backgrounds to $b\bar{b}$ production. The invariant mass of the dimuons is restricted to the range $6 < M^{\mu\mu} < 35$ GeV/c^2. The lower limit removes dimuons resulting from the cascade decay of single b-quarks and J/ψ decays, while the upper limit reduces dimuon decays of the Z boson. An opening angle cut of $\Delta\phi_{3D} < 165°$ between the muons is also applied to remove contamination from cosmic ray muons. A total of 397 events pass all selection criteria.

The trigger and offline reconstruction efficiencies, were determined by Monte Carlo. ISAJET (5) events were passed through a detailed GEANT (6) simulation of the detector and passed through full trigger simulation and reconstruction programs. Trigger and some offline efficiencies found in this way were cross checked by using appropriate data samples. The overall acceptance and efficiency as a function of the leading muon in the event increases from about 1% at 4 GeV/c to a plateau of 9% at 15 GeV/c. We define the leading muon in the event as the muon with the greater value of p_T^μ.

SIGNAL AND BACKGROUND DETERMINATION

In addition to $b\bar{b}$ production, dimuon events in the mass range 6-35 GeV/c^2 can also arise from other sources. These processes include semi-leptonic decays of $c\bar{c}$ pairs, events in which one or both of the muons are produced by in-flight decays of π or K mesons, Drell-Yan production, and Υ decays. Muons from Drell-Yan and Υ decays are not expected to have jets associated with them. Monte Carlo estimates normalized to the measured Drell-Yan and Υ cross sections (8) show that less than one event is expected to contribute to the final data sample from these two sources. An additional source of dimuons originates from cosmic ray muons passing through the detector.

To extract the $b\bar{b}$ signal, we used a maximum likelihood fit with four different input distributions. The input distributions were chosen based on their effectiveness in distinguishing

between the different sources of dimuon events. We used the transverse momentum of the muon with respect to the jet axis, p_T^{rel}, for both the leading and trailing muon, the fraction of longitudinal momentum of the jet carried by the leading muon divided by the jet E_T, z', and the reconstructed time of passage, t_0^f, of the leading muon track through the muon chambers with respect to the beam crossing time. The last variable, t_0^f, was used to subtract the cosmic ray muon background which is not expected to pass in time with the beam crossing. For both p_T^{rel} and z', the jet energy is defined to be the vector sum of the muon plus jet energies minus the expected minimum ionizing energy of the muon.

The p_T^{rel} and z' distributions for $b\overline{b}$, $c\overline{c}$, and b or c plus π/K decay were modeled using the ISAJET Monte Carlo. Each of these samples was processed with a complete detector, trigger, and offline simulation. The distributions for b-quark decays include both direct ($b \to \mu$) and sequential ($b \to c \to \mu$) decays. The distributions for $c\overline{c}$ and a c-quark plus a π or K decay are very similar, so the contributions from both of these processes was fit as a single process. The distributions for t_0^f were obtained from two different sources. The t_0^f distribution for cosmic ray muons was obtained during special runs where the detector triggered on cosmic rays. For beam produced muons, the t_0^f was calculated using muons from J/ψ decays.

Figure 1 shows the result of the maximum likelihood fit for p_T^{rel} of the leading and trailing muons. Included in Fig. 1 are the contributions from each of the sources of dimuon events. The $b\overline{b}$ contribution to the final data sample is found to be 45.3±5.8%. The other fraction of the data set is comprised of b or c plus π/K decay($37.9^{+5.5}_{-5.7}$%), $c\overline{c}$($14.0^{+3.9}_{-3.7}$%), and cosmic ray contamination($2.8^{+1.7}_{-1.5}$%). As a result of the fit, we obtain the number of $b\overline{b}$ events in each bin as a function of p_T^{μ} of the leading muon and as a function of the difference in azimuthal angle between the two muons, $\Delta\phi^{\mu\mu}$. The systematic errors on the number of $b\overline{b}$ events in each bin ($\simeq$ 8%) were estimated by varying the input distributions to the maximum likelihood fit. A complete description of the fitting procedure can be found in Ref. (7).

As a cross check to the fitting procedure, we calculate f_b, the fraction of events originating from $b\overline{b}$ production, using a Monte Carlo sample and compare this result to that determined by the maximum likelihood fit to the data. The Monte Carlo calculation of f_b applies all trigger and offline selection cuts and includes all sources of QCD dimuon events. In addition, the Monte Carlo sample cross sections are normalized to the next-to-leading order calculations of Ref. (2). Figure 2 shows good agreement between the Monte Carlo calculated fraction of dimuon events from $b\overline{b}$ production and what is found in the data.

RESULTS AND DISCUSSION

The dimuon cross section originating from $b\overline{b}$ production was calculated using

$$\frac{d\sigma_{b\overline{b}}^{\mu\mu}}{dp_T^{\mu_1}} = \frac{1}{\Delta p_T^{\mu_1}} \frac{N_{b\overline{b}} f_p}{\epsilon \int \mathcal{L} dt} \tag{1}$$

and

$$\frac{d\sigma_{b\overline{b}}^{\mu\mu}}{d\Delta\phi^{\mu\mu}} = \frac{1}{\Delta\phi^{\mu\mu}} \frac{N_{b\overline{b}} f_p}{\epsilon \int \mathcal{L} dt}, \tag{2}$$

where μ_1 refers to the leading muon in the event, and f_p is an unfolding factor to account for the smearing due to the muon momentum resolution. An unfolding technique (9) was

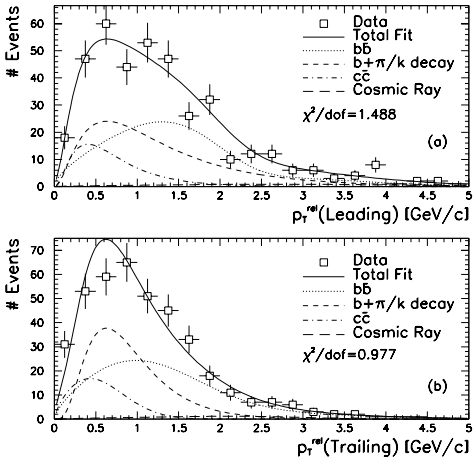

FIG. 1. The results of the maximum likelihood fit to the data for (a) p_T^{rel} of the leading muon and (b) p_T^{rel} of the trailing muon. Also included are the curves showing the contribution from each process to the dimuon sample.

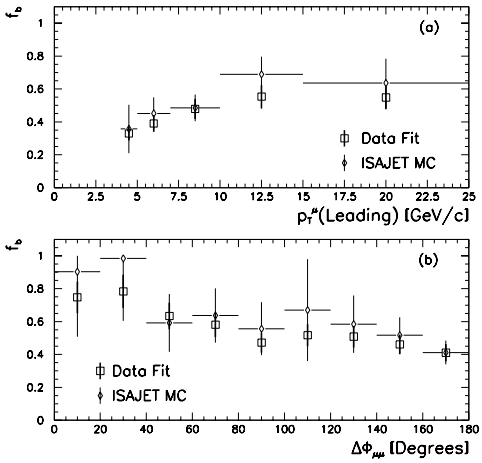

FIG. 2. The fraction of dimuon data associated with $b\overline{b}$ production, f_b, as a function of (a) p_T^{rel} of the leading muon and (b) $\Delta\phi^{\mu\mu}$. The open diamonds represent the Monte Carlo estimates to f_b.

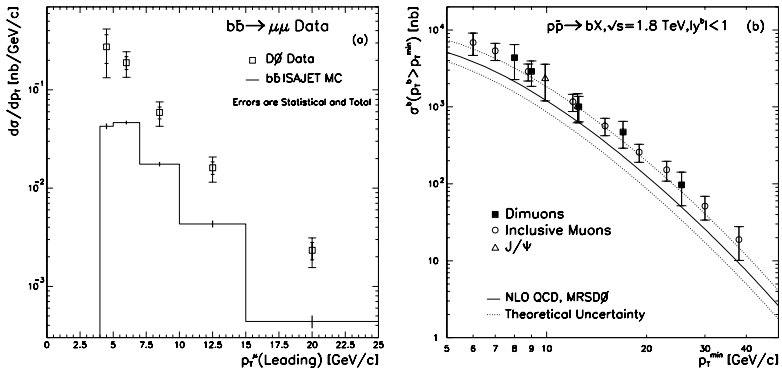

FIG. 3. (a) The unfolded $p_T^{\mu_1}$ spectrum for $b\overline{b}$ production compared to the expected spectrum (see text) where the data errors are statistical and total and the Monte Carlo errors are statistical only; (b) the b-quark production cross section compared with previous DØ results and the NLO QCD predictions. The error bars represent the total error.

used to determine f_p. f_p varies from ≈ 0.78 at low $p_T^{\mu_1}$ to ≈ 0.93 in the highest $p_T^{\mu_1}$ bin. The systematic uncertainty associated with f_p was estimated to be 43% in the low $p_T^{\mu_1}$ bin to $\approx 5\%$ in the highest$p_T^{\mu_1}$ bin.

Figure 3(a) shows the result of this calculation as a function of $p_T^{\mu_1}$. The $b\overline{b} \to \mu\mu$ cross section is shown for $4 < p_T^{\mu} < 25$ GeV/c, $|\eta^{\mu}| < 0.8$, $6 < M^{\mu\mu} < 35$ GeV/c^2, and $\Delta\phi_{3D} < 165°$. The total systematic error is found to be $p_T^{\mu_1}$ dependent, ranging from 18-48%. This includes uncertainties from trigger efficiency (19%), offline selection cuts (5%), likelihood fit (6%), and the integrated luminosity (5%). The theoretical $b\overline{b} \to \mu\mu$ curve was calculated using ISAJET for b-quark production with the CTEQ 2L parton distributions (10) and cross section normalized to the NLO QCD calculation (2).

To extract the b-quark cross section from the dimuon data, we employ a method first used by UA1 (11) and subsequently used by both CDF (12) and DØ (1). Since a correlation exists between the p_T of the muons produced from b-quark decays and the parent b-quark p_T, the muon p_T cuts in the data are effectively b-quark p_T cuts. For a set of kinematic cuts, including cuts on the transverse momentum of the muons, we define p_T^{min} as that value of the b-quark p_T such that 90% of the accepted events have b-quark transverse momentum greater than p_T^{min}. The b-quark cross section can then be calculated as

$$\sigma_b(p_T^b > p_T^{min}) = \sigma_{b\overline{b}}^{\mu\mu}(p_T^{\mu_1}) \frac{\sigma_b^{MC}}{\sigma_{b\overline{b}\to\mu\mu}^{MC}}, \tag{3}$$

where $\sigma_{b\overline{b}}^{\mu\mu}(p_T^{\mu_1})$ is the measured integrated dimuon cross section of Eq. (1) integrated over different intervals of $p_T^{\mu_1}$, σ_b^{MC} is the total Monte Carlo b-quark cross section for $p_T^b > p_T^{min}$, and $\sigma_{b\overline{b}\to\mu\mu}^{MC}$ is the Monte Carlo cross section for dimuon production with cuts that match the data set. For each interval of $p_T^{\mu_1}$, p_T^{min} is calculated using ISAJET. Additional uncertainties incurred when extracting the b-quark cross section include B-hadron leptonic branching fraction (7%), parameterization in the fragmentation (20%), and muon decay spectrum

(11%). Combining these errors with those on the dimuon cross section, we obtain a total systematic uncertainty of 35-48% on the b-quark cross section.

The results of the b-quark production cross section as a function of p_T^{min}, for $|y^b| < 1.0$, are shown in Fig. 3(b). Also included are previous measurements of the b-quark cross section measured by DØ (1). The two curves represent the NLO QCD predictions (2) using $m_b = 4.75$ GeV/c^2 and the MRSD0 (13) structure functions with $\Lambda^5_{\overline{MS}} = 140$ MeV. The theoretical uncertainty results from varying the QCD mass scale between 100< $\Lambda^5_{\overline{MS}}$ <187 MeV and the factorization and renormalization scale, μ, in the range $\mu_0/2 < \mu < 2\mu_0$, where $\mu_0^2 = m_b^2 + \langle p_T^b \rangle^2$.

The differential $b\overline{b}$ cross section calculated in Eq. (2) gives further information on the underlying QCD production mechanisms by studying the topological correlation between the two b-quarks. The difference between the azimuthal angle between the b and $\overline{b}$-quarks(or equivalently, between the decay muons), allows us to differentiate between the contributing QCD production mechanisms. These contributions include the leading order term, flavor creation, and the two next-to-leading order terms, gluon splitting and flavor excitation. There are also contributions from interference terms.

The cross section $d\sigma^{\mu\mu}_{b\overline{b}}/d\Delta\phi^{\mu\mu}$ is shown in Fig. 4 after acceptance correction for the three-dimensional opening angle cut. Also shown is the NLO QCD prediction that we have determined using the HVQJET Monte Carlo. HVQJET is a direct implementation of the NLO MNR calculation which uses a modified version of ISAJET for hadronization, particle decays, and modeling of the underlying event. In HVQJET, the MNR prediction is realized by combining troublesome parton level events having negative weights with parton level events having positive weights but similar topologies. The prediction shown in Fig. 4 includes only gluon-gluon initiated subprocesses but other subprocess contributions are expected to be small.

The data show a clear excess above the HVQJET prediction but agree with the overall shape. The ratio between the data and the $\Delta\phi^{\mu\mu}_{MNR}$ calculation is shown in Fig. 4. A zero-order polynomial fit to this ratio indicates that the data differ from the NLO theoretical calculation by an overall constant of 1.9±0.2.

CONCLUSIONS

In conclusion, we have measured both the b-quark production cross section and the azimuthal correlations between the two b-quarks using dimuons to tag the presence of b-quarks. Both measurements are found to agree in shape with the NLO QCD calculation of heavy flavor production but lie above the central values of these predictions (yet within the theoretical uncertainties).

ACKNOWLEDGMENTS

We thank the staffs at Fermilab and the collaborating institutions for their contributions to the success of this work, and acknowledge support from the Department of Energy and National Science Foundation (U.S.A.), Commissariat à L'Energie Atomique (France), Ministries for Atomic Energy and Science and Technology Policy (Russia), CNPq (Brazil), Departments of Atomic Energy and Science and Education (India), Colciencias (Colombia), CONACyT (Mexico), Ministry of Education and KOSEF (Korea), CONICET and UBACyT (Argentina), and the A.P. Sloan Foundation.

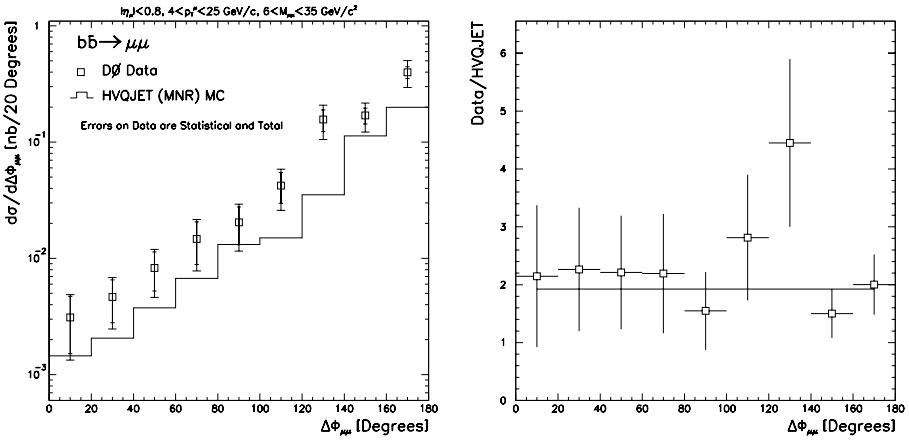

FIG. 4. (a) The $\Delta\phi^{\mu\mu}$ spectrum for $b\overline{b}$ production compared to the HVQJET prediction (see text); (b) the ratio between the data spectrum and the HVQJET prediction of Fig. 4(a). Also shown is a zero-order polynomial fit to this ratio.

REFERENCES

1. DØ Collaboration, S. Abachi *et al.*, Phys. Rev. Lett. **74**, 3548 (1995), Phys. Lett. B **370**, 239 (1996).
2. P. Nason, S. Dawson, and R.K. Ellis, Nucl. Phys. **B327**, 49 (1989).
3. M. Mangano, P. Nason, and G. Ridolfi, Nucl. Phys. **B373**, 295 (1992).
4. DØ Collaboration, S. Abachi *et al.*, Nucl. Instrum. Methods Phys. Res., Sect. A **338**, 185 (1994).
5. F. Paige and S. Protopopescu, BNL Report No. BNL38034, 1986 (unpublished), release v 7.0.
6. F. Carminati *et al.*, "GEANT Users Guide", v 3.15, CERN Program Library, December, 1991 (unpublished).
7. D. Fein, Ph.D. Thesis, University of Arizona (1996), unpublished.
8. A. Smith, Ph.D. Thesis, University of Arizona (1996), unpublished.
9. G.D'Agostini, DESY Report No. 94-099, 1994.
10. CTEQ Collaboration, J. Botts *et al.*, Phys. Lett. B **304**, 159 (1993).
11. UA1 Collaboration, C. Albajar *et al.*, Phys. Lett. B **256**, 121 (1991).
12. CDF Collaboration, F. Abe *et al.*, Phys. Rev. Lett. **68**, 2403 (1992), **69**, 3704 (1992), **71**, 500 (1993), **71**, 2396 (1993), **71**, 2537 (1993).
13. A. Martin, R. Roberts, and J.W. Sterling, Phys. Rev. D **47**, 867 (1993).